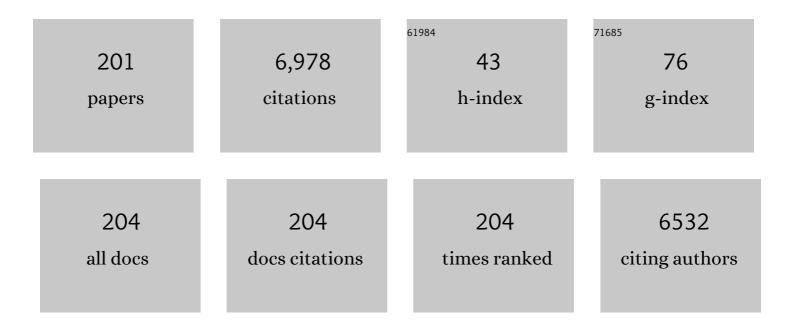
Andre Stesmans

List of Publications by Year in descending order

Source: https://exaly.com/author-pdf/1693492/publications.pdf Version: 2024-02-01



#	Article	IF	CITATIONS
1	Strain-induced semiconductor to metal transition in the two-dimensional honeycomb structure of MoS2. Nano Research, 2012, 5, 43-48.	10.4	620
2	Electronic properties of hydrogenated silicene and germanene. Applied Physics Letters, 2011, 98, .	3.3	399
3	Internal photoemission at interfaces of high-l [°] insulators with semiconductors and metals. Journal of Applied Physics, 2007, 102, .	2.5	223
4	Can silicon behave like graphene? A first-principles study. Applied Physics Letters, 2010, 97, .	3.3	208
5	Structural relaxation ofPbdefects at the (111)Si/SiO2interface as a function of oxidation temperature: ThePb-generation–stress relationship. Physical Review B, 1993, 48, 2418-2435.	3.2	192
6	Band alignments in metal–oxide–silicon structures with atomic-layer deposited Al2O3 and ZrO2. Journal of Applied Physics, 2002, 91, 3079-3084.	2.5	190
7	Electron spin resonance features of interface defects in thermal (100)Si/SiO2. Journal of Applied Physics, 1998, 83, 2449-2457.	2.5	164
8	Vibrational properties of silicene and germanene. Nano Research, 2013, 6, 19-28.	10.4	144
9	Dissociation kinetics of hydrogen-passivatedPbdefects at the(111)Si/SiO2interface. Physical Review B, 2000, 61, 8393-8403.	3.2	120
10	Interface traps and dangling-bond defects in (100)Geâ^•HfO2. Applied Physics Letters, 2005, 87, 032107.	3.3	119
11	First-principles study of strained 2D MoS2. Physica E: Low-Dimensional Systems and Nanostructures, 2014, 56, 416-421.	2.7	119
12	Elimination of SiC/SiO2 interface states by preoxidation ultravioletâ€ozone cleaning. Applied Physics Letters, 1996, 68, 2141-2143.	3.3	116
13	Electronic properties of two-dimensional hexagonal germanium. Applied Physics Letters, 2010, 96, .	3.3	114
14	Electrical activity of interfacial paramagnetic defects in thermal (100)Si/SiO2. Physical Review B, 1998, 57, 10030-10034.	3.2	111
15	Interfacial Defects in SiO2Revealed by Photon Stimulated Tunneling of Electrons. Physical Review Letters, 1997, 78, 2437-2440.	7.8	107
16	Energy band alignment at the (100)Ge/HfO2 interface. Applied Physics Letters, 2004, 84, 2319-2321.	3.3	107
17	Synthesis and characterization of sol-gel derived ZnS : Mn2+ nanocrystallites embedded in a silica matrix. Bulletin of Materials Science, 2002, 25, 175-180.	1.7	105
18	Interaction of Pb defects at the (111)Si/SiO2 interface with molecular hydrogen: Simultaneous action of passivation and dissociation. Journal of Applied Physics, 2000, 88, 489-497.	2.5	99

#	Article	IF	CITATIONS
19	Si dangling-bond-type defects at the interface of (100)Si with ultrathin layers of SiOx, Al2O3, and ZrO2. Applied Physics Letters, 2002, 80, 1957-1959.	3.3	92
20	Si dangling-bond-type defects at the interface of (100)Si with ultrathin HfO2. Applied Physics Letters, 2003, 82, 4074-4076.	3.3	91
21	Low temperature silicon dioxide by thermal atomic layer deposition: Investigation of material properties. Journal of Applied Physics, 2010, 107, .	2.5	86
22	Characterization and depth profiling ofE' defects in buried SiO2. Journal of Applied Physics, 1993, 74, 275-283.	2.5	81
23	Decreased Recombination Through the Use of a Nonâ€Fullerene Acceptor in a 6.4% Efficient Organic Planar Heterojunction Solar Cell. Advanced Energy Materials, 2014, 4, 1301413.	19.5	75
24	Stable trapping of electrons and holes in deposited insulating oxides: Al2O3, ZrO2, and HfO2. Journal of Applied Physics, 2004, 95, 2518-2526.	2.5	74
25	Thermally induced interface degradation in (111) Si/SiO2traced by electron spin resonance. Physical Review B, 1996, 54, R11129-R11132.	3.2	72
26	Degradation of the thermal oxide of the Si/SiO2/Al system due to vacuum ultraviolet irradiation. Journal of Applied Physics, 1995, 78, 6481-6490.	2.5	65
27	Alternative techniques to reduce interface traps in nâ€ŧype 4H‣iC MOS capacitors. Physica Status Solidi (B): Basic Research, 2008, 245, 1378-1389.	1.5	64
28	Influence of interface relaxation on passivation kinetics in H2 of coordination Pb defects at the (111)Si/SiO2 interface revealed by electron spin resonance. Journal of Applied Physics, 2002, 92, 1317-1328.	2.5	63
29	Conduction band-edge States associated with the removal of d-state degeneracies by the Jahn-Teller effect. IEEE Transactions on Device and Materials Reliability, 2005, 5, 65-83.	2.0	63
30	Electrical Characterization of Ultrathin RF-Sputtered LiPON Layers for Nanoscale Batteries. ACS Applied Materials & Interfaces, 2016, 8, 7060-7069.	8.0	63
31	Interface state energy distribution and Pb defects at Si(110)/SiO2 interfaces: Comparison to (111) and (100) silicon orientations. Journal of Applied Physics, 2011, 109, .	2.5	61
32	Controlled Sulfurization Process for the Synthesis of Large Area MoS ₂ Films and MoS ₂ /WS ₂ Heterostructures. Advanced Materials Interfaces, 2016, 3, 1500635.	3.7	61
33	High Cycling Stability and Extreme Rate Performance in Nanoscaled LiMn ₂ O ₄ Thin Films. ACS Applied Materials & Interfaces, 2015, 7, 22413-22420.	8.0	59
34	Two-Dimensional Crystal Grain Size Tuning in WS ₂ Atomic Layer Deposition: An Insight in the Nucleation Mechanism. Chemistry of Materials, 2018, 30, 7648-7663.	6.7	57
35	Reaction-dispersive proton transport model for negative bias temperature instabilities. Applied Physics Letters, 2005, 86, 093506.	3.3	51
36	Influence of Al ₂ O ₃ crystallization on band offsets at interfaces with Si and TiN _x . Applied Physics Letters, 2011, 99, 072103.	3.3	50

#	Article	IF	CITATIONS
37	Electron states and microstructure of thina-C:H layers. Physical Review B, 1996, 54, 10820-10826.	3.2	49
38	Vibrational properties of epitaxial silicene layers on (111) Ag. Applied Surface Science, 2014, 291, 113-117.	6.1	49
39	Hole traps in oxide layers thermally grown on SiC. Applied Physics Letters, 1996, 69, 2252-2254.	3.3	47
40	Thermally induced interface degradation in (100) and (111) Si/SiO[sub 2] analyzed by electron spin resonance. Journal of Vacuum Science & Technology an Official Journal of the American Vacuum Society B, Microelectronics Processing and Phenomena, 1998, 16, 3108.	1.6	47
41	The origin of white luminescence from silicon oxycarbide thin films. Applied Physics Letters, 2014, 104,	3.3	45
42	Hydrogen-induced thermal interface degradation in (111) Si/SiO2 revealed by electron-spin resonance. Applied Physics Letters, 1998, 72, 2271-2273.	3.3	44
43	Ruthenium gate electrodes on SiO2 and HfO2: Sensitivity to hydrogen and oxygen ambients. Applied Physics Letters, 2006, 88, 243514.	3.3	44
44	Nitrogen at the <mml:math <br="" xmlns:mml="http://www.w3.org/1998/Math/MathML">display="inline"><mml:mrow><mml:mtext>Si-nanocrystal</mml:mtext><mml:mo>/</mml:mo><mml:msub><mr and its influence on luminescence and interface defects. Physical Review B, 2010, 82, .</mr </mml:msub></mml:mrow></mml:math>	nl:13120w>	<m##:mtext></m##:mtext>
45	On the chemistry and electrochemistry of LiPON breakdown. Journal of Materials Chemistry A, 2018, 6, 4848-4859.	10.3	44
46	Semiconducting-like filament formation in TiN/HfO2/TiN resistive switching random access memories. Applied Physics Letters, 2012, 100, .	3.3	43
47	H-complexed oxygen vacancy in SiO2: Energy level of a negatively charged state. Applied Physics Letters, 1997, 71, 3844-3846.	3.3	42
48	High open-circuit voltage values on fine-grained thin-film polysilicon solar cells. Journal of Applied Physics, 2006, 100, 063702.	2.5	41
49	Pb(0) centers at the Si-nanocrystal/SiO2 interface as the dominant photoluminescence quenching defect. Journal of Applied Physics, 2010, 107, 084309.	2.5	41
50	Hole-Doped 2D InSe for Spintronic Applications. ACS Applied Nano Materials, 2018, 1, 6656-6665.	5.0	41
51	Positive charging of thermal SiO2/(100)Si interface by hydrogen annealing. Applied Physics Letters, 1998, 72, 79-81.	3.3	40
52	Annealing induced degradation of thermal SiO2: S center generation. Applied Physics Letters, 1996, 69, 2056-2058.	3.3	39
53	Generation aspects of the delocalized intrinsicEXdefect in thermal SiO2. Journal of Applied Physics, 1994, 75, 1047-1058.	2.5	38
54	Maximum density ofPbcenters at the (111) Si/SiO2interface after vacuum anneal. Applied Physics Letters, 1990, 57, 2663-2665.	3.3	37

#	Article	IF	CITATIONS
55	Hydrogenâ€Related Leakage Currents Induced in Ultrathin SiO2 / Si Structures by Vacuum Ultraviolet Radiation. Journal of the Electrochemical Society, 1999, 146, 3409-3414.	2.9	37
56	Paramagnetic defects at the interface of ultrathin oxides grown under vacuum ultraviolet photon excitation on (111) and (100) Si. Applied Physics Letters, 2000, 77, 1469-1471.	3.3	35
57	Valence band offset and hole injection at the 4H-, 6H-SiC/SiO2 interfaces. Applied Physics Letters, 2000, 77, 2024-2026.	3.3	35
58	Hole trapping in ultrathin Al2O3 and ZrO2 insulators on silicon. Applied Physics Letters, 2002, 80, 1261-1263.	3.3	35
59	TiN x / HfO 2 interface dipole induced by oxygen scavenging. Applied Physics Letters, 2011, 98, .	3.3	34
60	Defect generation in high $\hat{\mathbf{l}}^{\mathrm{g}}$ gate dielectric stacks under electrical stress: the impact of hydrogen. Journal of Physics Condensed Matter, 2005, 17, S2075-S2088.	1.8	33
61	Positive charging of buried SiO2by hydrogenation. Applied Physics Letters, 1994, 64, 2575-2577.	3.3	32
62	Model for the charge trapping in high permittivity gate dielectric stacks. Journal of Applied Physics, 2001, 89, 792-794.	2.5	32
63	Topological to trivial insulating phase transition in stanene. Nano Research, 2016, 9, 774-778.	10.4	32
64	A theoretical study of the initial oxidation of the GaAs(001)-β2(2×4) surface. Applied Physics Letters, 2009, 95, .	3.3	31
65	Band alignment at interfaces of few-monolayer MoS2 with SiO2 and HfO2. Microelectronic Engineering, 2015, 147, 294-297.	2.4	31
66	Silicene on non-metallic substrates: Recent theoretical and experimental advances. Nano Research, 2018, 11, 1169-1182.	10.4	31
67	Chemical etch rates in HF solutions as a function of thickness of thermal SiO2and buried SiO2formed by oxygen implantation. Journal of Applied Physics, 1991, 69, 6656-6664.	2.5	30
68	Energy distribution of the (100)Si/HfO2 interface states. Applied Physics Letters, 2004, 84, 4771-4773.	3.3	30
69	Energy barriers at interfaces of (100)GaAs with atomic layer deposited Al2O3 and HfO2. Applied Physics Letters, 2008, 93, .	3.3	30
70	Structural Properties of Al–O Monolayers in SiO ₂ on Silicon and the Maximization of Their Negative Fixed Charge Density. ACS Applied Materials & Interfaces, 2018, 10, 30495-30505.	8.0	30
71	Effective work function modulation by controlled dielectric monolayer deposition. Applied Physics Letters, 2006, 89, 113505.	3.3	29
79	Nontrigonal Ge dangling bond interface defect in condensation-grown <mml:math xmlns:mml="http://www.w3.org/1998/Math/MathML"</mml:math 	Q ()	28

72 display="inline"><mml:mrow><mml:mrow><mml:mo>(</mml:mo><mml:mrow><mml:mrow><mml:mn>100</mml:mn></mml:mirow><mml:mo>)</m Physical Review B, 2009, 79, .

#	Article	IF	CITATIONS
73	Observation of a delocalizedE' center in buried SiO2. Applied Physics Letters, 1993, 62, 2405-2407.	3.3	26
74	Electronic structure of the interface of aluminum nitride with Si(100). Journal of Applied Physics, 2008, 104, 093713.	2.5	25
75	Impact of point defects on the electronic and transport properties of silicene nanoribbons. Journal of Physics Condensed Matter, 2016, 28, 035302.	1.8	25
76	Energy barriers at interfaces between (100) InxGa1â^'xAsâ€^(â‰ ¤ â‰ 0 .53) and atomic-layer deposited Al2O3 and HfO2. Applied Physics Letters, 2009, 94, .	3.3	24
77	Advances in SiCN-SiCN Bonding with High Accuracy Wafer-to-Wafer (W2W) Stacking Technology. , 2018, , .		24
78	Invasive nature of corona charging on thermal Si/SiO2 structures with nanometer-thick oxides revealed by electron spin resonance. Applied Physics Letters, 2003, 82, 2835-2837.	3.3	23
79	Paramagnetic point defects at SiO2/nanocrystalline Si interfaces. Applied Physics Letters, 2008, 93, .	3.3	22
80	Ferromagnetism in two-dimensional hole-doped SnO. AIP Advances, 2018, 8, .	1.3	22
81	Improved cathode buffer layer to decrease exciton recombination in organic planar heterojunction solar cells. Applied Physics Letters, 2013, 102, .	3.3	21
82	Transitivity of band offsets between semiconductor heterojunctions and oxide insulators. Applied Physics Letters, 2011, 99, .	3.3	20
83	Contact Resistance at MoS ₂ -Based 2D Metal/Semiconductor Lateral Heterojunctions. ACS Applied Nano Materials, 2019, 2, 760-766.	5.0	19
84	Evidence for a phase-transition-induced change in the surface spin-flip probability of conduction electrons from CESR on n-irradiated, LIF; its application as an intensity reference. Journal Physics D: Applied Physics, 1988, 21, 1205-1214.	2.8	18
85	Electron-spin-resonance analysis of the natural intrinsicEXcenter in thermalSiO2on Si. Physical Review B, 1995, 51, 4987-4997.	3.2	18
86	Valence band energy in confined Si1â^'xGex (0.28 <x<0.93) 172106.<="" 2009,="" 94,="" applied="" layers.="" letters,="" physics="" td=""><td>3.3</td><td>18</td></x<0.93)>	3.3	18
87	Oxidation of the GaAs(001) surface: Insights from first-principles calculations. Physical Review B, 2012, 85, .	3.2	18
88	Functional silicene and stanene nanoribbons compared to graphene: electronic structure and transport. 2D Materials, 2016, 3, 015001.	4.4	18
89	Paramagnetic point defects at interfacial layers in biaxial tensile strained (100)Si/SiO2. Journal of Applied Physics, 2008, 103, .	2.5	17
90	Electronic properties of Ge dangling bond centers at Si1â^'xGex/SiO2 interfaces. Applied Physics Letters, 2009, 95, 222106.	3.3	17

#	Article	lF	CITATIONS
91	Electron band alignment between (100)InP and atomic-layer deposited Al2O3. Applied Physics Letters, 2010, 97, 132112.	3.3	17
92	Electrically active defects at AlN/Si interface studied by DLTS and ESR. Physica Status Solidi (A) Applications and Materials Science, 2012, 209, 1851-1856.	1.8	17
93	Band alignment at interfaces of synthetic few-monolayer MoS2 with SiO2 from internal photoemission. APL Materials, 2018, 6, .	5.1	17
94	Beneficial effect of La on band offsets in Ge/high- \hat{I}° insulator structures with GeO2 and La2O3 interlayers. Applied Physics Letters, 2008, 93, 102115.	3.3	16
95	Correlation between interface traps and paramagnetic defects in c-Si/a-Si:H heterojunctions. Applied Physics Letters, 2012, 100, .	3.3	15
96	High-resolution electron spin resonance analysis of ion bombardment induced defects in advanced low-l̂º insulators (l̂ºâ€‰= 2.0-2.5). Applied Physics Letters, 2013, 102, .	3.3	15
97	Ferromagnetism and half-metallicity in two-dimensional <mml:math xmlns:mml="http://www.w3.org/1998/Math/MathML"><mml:mrow><mml:mi>M</mml:mi><mml:mi mathvariant="normal">O<mml:mo>Â</mml:mo><mml:mo>(</mml:mo><mml:mi>M</mml:mi><mml: monolayers induced by hole doping. Physical Review Materials, 2020, 4, .</mml: </mml:mi </mml:mrow></mml:math 	no?:4 no?:= <td>nl:150><mml< td=""></mml<></td>	nl:150> <mml< td=""></mml<>
98	The application of submetallic phosphorus-doped Si as ESR marker. Journal of Magnetic Resonance, 1988, 76, 14-21.	0.5	14
99	Reducing exciton-polaron annihilation in organic planar heterojunction solar cells. Physical Review B, 2014, 90, .	3.2	14
100	ESR study of p-type natural 2H-polytype MoS2 crystals: The As acceptor activity. Applied Physics Letters, 2016, 109, .	3.3	14
101	Internal Photoemission Metrology of Inhomogeneous Interface Barriers. Physica Status Solidi (A) Applications and Materials Science, 2018, 215, 1700865.	1.8	14
102	Contact resistance at graphene/MoS2 lateral heterostructures. Applied Physics Letters, 2019, 114, .	3.3	14
103	ESR and Photo-ESR Study of Defects in CVD Diamond. Physica Status Solidi A, 2002, 193, 448-456.	1.7	13
104	Magnetic Properties of Substituted Poly(thiophene)s in Their Neutral State. Macromolecules, 2010, 43, 2910-2915.	4.8	13
105	Shallow donor in separation by implantation of oxygen structures revealed by electricâ€field modulated electron spin resonance. Applied Physics Letters, 1993, 62, 273-275.	3.3	12
106	Photoconductivity of Hf-based binary metal oxide systems. Journal of Applied Physics, 2008, 104, 114103.	2.5	12
107	Current-voltage characteristics of armchair Sn nanoribbons. Physica Status Solidi - Rapid Research Letters, 2014, 8, 931-934.	2.4	12
108	Paramagnetic Intrinsic Defects in Polycrystalline Large-Area 2D MoS2 Films Grown on SiO2 by Mo Sulfurization. Nanoscale Research Letters, 2017, 12, 283.	5.7	12

#	Article	IF	CITATIONS
109	(Invited) Internal Photoemission of Electrons from 2-Dimensional Semiconductors. ECS Transactions, 2017, 80, 191-201.	0.5	12
110	Aryl-viologen pentapeptide self-assembled conductive nanofibers. Chemical Communications, 2019, 55, 7354-7357.	4.1	12
111	Two-dimensional gallium and indium oxides from global structure searching: Ferromagnetism and half metallicity via hole doping. Journal of Applied Physics, 2020, 128, 034304.	2.5	12
112	Electron spin resonance characterization and localization of a thermally generated donor inherent to the separation by implantation of oxygen process. Journal of Applied Physics, 1993, 73, 876-889.	2.5	11
113	Defects at the interface of (100)Si with ultrathin layers of SiO[sub x], Al[sub 2]O[sub 3], and ZrO[sub 2] probed by electron spin resonance. Journal of Vacuum Science & Technology an Official Journal of the American Vacuum Society B, Microelectronics Processing and Phenomena, 2002, 20, 1720.	1.6	11
114	Electron energy band alignment at the (100)Si/MgO interface. Applied Physics Letters, 2010, 96, .	3.3	11
115	Influence of <i>in situ</i> applied ultrasound during Si+ implantation in SiO2 on paramagnetic defect generation. Journal of Applied Physics, 2010, 107, .	2.5	11
116	First-principles study of Ge dangling bonds in GeO2 and correlation with electron spin resonance at Ge/GeO2 interfaces. Applied Physics Letters, 2011, 99, .	3.3	11
117	Electron band alignment at the interface of (100)InSb with atomic-layer deposited Al ₂ O ₃ . Applied Physics Letters, 2012, 101, 082114.	3.3	11
118	Influence of the bulkiness of the substituent on the aggregation and magnetic properties of poly(3â€alkylthiophene)s. Journal of Polymer Science Part A, 2014, 52, 76-86.	2.3	11
119	Energy Band Alignment of a Monolayer MoS 2 with SiO 2 and Al 2 O 3 Insulators from Internal Photoemission. Physica Status Solidi (A) Applications and Materials Science, 2019, 216, 1800616.	1.8	11
120	Impact of MoS ₂ layer transfer on electrostatics of MoS ₂ /SiO ₂ interface. Nanotechnology, 2019, 30, 055702.	2.6	11
121	Electrical conduction of buried SiO2 layers analyzed by photon stimulated electron tunneling. Applied Physics Letters, 1997, 70, 1260-1262.	3.3	10
122	Vacancy clusters in diamond studied by electron spin resonance. Physica Status Solidi A, 2004, 201, 2509-2515.	1.7	10
123	First-principles study of the electronic properties of Ge dangling bonds at (100)Si1â^'xGex/SiO2 interfaces. Applied Physics Letters, 2009, 95, .	3.3	10
124	Electron spin resonance observation of an interfacial Ge <i>P</i> _{<i>b</i>1} -type defect in SiO ₂ <i>/</i> (100)Si _{1â^²<i>x</i>} Ge _{<i>x</i>} Ce _{<i>/</i>} <i>/<i>/Ce_{<i>/</i>}<i>/<i>/Ce<sub>Ce<sub>Ce<sub>Ce<sub>Ce<sub>Ce<sub>Ce<sub>Ce<sub>Ce<sub>Ce<sub>Ce<sub>Ce<sub>Ce<sub>Ce<sub>Ce<sub>Ce<sub>Ce<sub>Ce<sub>Ce<sub>Ce<sub>Ce<sub>Ce<sub>Ce<sub>Ce<sub>Ce<sub>Ce<sub>Ce<sub>Ce<sub>Ce<sub>Ce<sub>Ce<sub>Ce<sub>Ce<sub>Ce<sub>Ce<sub>Ce<sub>Ce<sub>Ce<sub>Ce<sub>Ce<sub>Ce<sub>Ce<sub>Ce<sub>Ce<sub>Ce<sub>Ce<sub>Ce<sub>Ce<sub>Ce<sub>Ce<sub>Ce<sub>Ce<sub>Ce<sub>Ce<sub>Ce<sub>Ce<sub>Ce<sub>Ce<sub>Ce<sub>Ce<sub>Ce<sub>Ce<sub>Ce<sub>Ce<sub>Ce<sub>Ce<sub>Ce<sub>Ce<sub>Ce<sub>Ce<sub>Ce<sub>Ce<sub>Ce<sub>Ce<sub>Ce<sub<se<sub>Ce<sub<se<sub>Ce<sub<se<sub>Ce<sub<se<sub>Ce<sub<se<sub>Ce<sub<se<sub>Ce<sub<se<sub<se<sub>Ce<sub<se<sub<se<sub<se<sub<se<sub<se<sub<se<sub<se<sub<se<sub<se<sub<se<sub<se<sub<se<sub>Ce<sub<se<sub<se<sub<se<sub<se<sub<se<sub<se<sub<se<sub<se<sub<se<sub<se<sub<se<sub<se<sub<se<sub<se<sub<se<sub>Ce<sub<se<sub<se<sub<se<sub<se<sub<se<sub<se<sub<se<sub<se<sub<se<sub<se<sub<se<sub<se<sub<se<sub<se<sub<se<sub<se<sub<se<sub<se<sub<se<sub<se<sub<se<sub<se<sub<se<sub<se<sub<se<sub<se<sub<se<sub<se<sub<se<sub<se<sub<se<sub<se<sub<se<sub<se<sub<se<sub<se<sub<se<sub<se<sub<se<sub<se<sub<se<sub<se<sub<se<sub<se<sub<se<sub<se<sub<se<sub<se<sub<se<sub<se<sub<se<sub<se<sub<se<sub<se<sub<se<sub<se<sub<se<sub<se<sub<se<sub<se<sub<se<sub<se<sub<se<sub<se<sub<se<sub<se<sub<se<sub<se<sub<se<sub<se<sub<se<sub<se<sub<se<sub<se<sub<se<sub<se<sub<se<sub<se<sub<se<sub<se<sub<se<sub<se<sub<se<sub<se<sub<se<sub<se<sub<se<sub<se<sub<se<sub<se<sub<se<sub<se<sub<se<sub<se<sub<se<sub<se<sub<se<sub<se<sub<se<sub<se<sub<se<sub<se<sub<se<sub<se<sub<se<sub<se<sub<se<sub<se<sub<se<sub<se<sub<se<sub<se<sub<se<sub<se<sub<se<sub<se<sub<se<sub<se<sub<se<sub<se<sub<se<sub<se<sub<se<sub<se<sub<se<sub<se<sub<se<sub<se<sub<se<sub<se<sub<se<sub<se<sub<se<sub<se<sub<se<sub<se<sub<se<sub<se<sub< td=""><td>i1.Si</td><td>10</td></sub<se<sub<se<sub<se<sub<se<sub<se<sub<se<sub<se<sub<se<sub<se<sub<se<sub<se<sub<se<sub<se<sub<se<sub<se<sub<se<sub<se<sub<se<sub<se<sub<se<sub<se<sub<se<sub<se<sub<se<sub<se<sub<se<sub<se<sub<se<sub<se<sub<se<sub<se<sub<se<sub<se<sub<se<sub<se<sub<se<sub<se<sub<se<sub<se<sub<se<sub<se<sub<se<sub<se<sub<se<sub<se<sub<se<sub<se<sub<se<sub<se<sub<se<sub<se<sub<se<sub<se<sub<se<sub<se<sub<se<sub<se<sub<se<sub<se<sub<se<sub<se<sub<se<sub<se<sub<se<sub<se<sub<se<sub<se<sub<se<sub<se<sub<se<sub<se<sub<se<sub<se<sub<se<sub<se<sub<se<sub<se<sub<se<sub<se<sub<se<sub<se<sub<se<sub<se<sub<se<sub<se<sub<se<sub<se<sub<se<sub<se<sub<se<sub<se<sub<se<sub<se<sub<se<sub<se<sub<se<sub<se<sub<se<sub<se<sub<se<sub<se<sub<se<sub<se<sub<se<sub<se<sub<se<sub<se<sub<se<sub<se<sub<se<sub<se<sub<se<sub<se<sub<se<sub<se<sub<se<sub<se<sub<se<sub<se<sub<se<sub<se<sub<se<sub<se<sub<se<sub<se<sub<se<sub<se<sub<se<sub<se<sub<se<sub<se<sub<se<sub<se<sub<se<sub<se<sub<se<sub<se<sub<se<sub<></sub<se<sub<se<sub<se<sub<se<sub<se<sub<se<sub<se<sub<se<sub<se<sub<se<sub<se<sub<se<sub<se<sub<se<sub<se<sub></sub<se<sub<se<sub<se<sub<se<sub<se<sub<se<sub<se<sub<se<sub<se<sub<se<sub<se<sub<se<sub></sub<se<sub<se_{</sub<se_{</sub<se_{</sub<se_{</sub<se_{</sub<se_{</sub<se}}}}}}</sub></sub></sub></sub></sub></sub></sub></sub></sub></sub></sub></sub></sub></sub></sub></sub></sub></sub></sub></sub></sub></sub></sub></sub></sub></sub></sub></sub></sub></sub></sub></sub></sub></sub></sub></sub></sub></sub></sub></sub></sub></sub></sub></sub></sub></sub></sub></sub></sub></sub></sub></sub></sub></sub></sub></sub></sub></sub></sub></sub></sub></sub></sub></sub></sub></sub></sub></i></i></i></i>	i1 .Si	10
125	Universal stress-defect correlation at (100)semiconductor/oxide interfaces. Applied Physics Letters, 2011, 98, 141901.	3.3	10
126	Magnetic defects in chemically converted graphene nanoribbons: electron spin resonance investigation. AIP Advances, 2014, 4, .	1.3	10

#	Article	IF	CITATIONS
127	Photonic nanostructures for advanced light trapping in silicon solar cells: the impact of etching on the material electronic quality. Physica Status Solidi - Rapid Research Letters, 2016, 10, 158-163.	2.4	10
128	ESR identification of the nitrogen acceptor in 2H-polytype synthetic MoS2: Dopant level and activation. AIP Advances, 2017, 7, 105006.	1.3	10
129	The lead acceptor in p-type natural 2H-polytype MoS ₂ crystals evidenced by electron paramagnetic resonance. Journal of Physics Condensed Matter, 2017, 29, 08LT01.	1.8	10
130	Band alignment at interfaces of two-dimensional materials: internal photoemission analysis. Journal of Physics Condensed Matter, 2020, 32, 413002.	1.8	10
131	Dissimilarity between thermal oxide and buried oxide fabricated by implantation of oxygen on Si revealed by etch rates in HF. Applied Physics Letters, 1990, 57, 2250-2252.	3.3	9
132	Defect generation sensitivity depth profile in buried SiO2using Ar plasma exposure. Applied Physics Letters, 1993, 62, 2277-2279.	3.3	9
133	Interface barriers at the interfaces of polar GaAs(111) faces with Al2O3. Applied Physics Letters, 2012, 100, .	3.3	9
134	Effect of Binder Content in Cu–In–Se Precursor Ink on the Physical and Electrical Properties of Printed CuInSe ₂ Solar Cells. Journal of Physical Chemistry C, 2014, 118, 27201-27209.	3.1	9
135	Analysis of Transferred MoS ₂ Layers Grown by MOCVD: Evidence of Mo Vacancy Related Defect Formation. ECS Journal of Solid State Science and Technology, 2020, 9, 093001.	1.8	9
136	Pressure dependence of Si/SiO2 degradation suppression by helium. Journal of Applied Physics, 2000, 87, 7338-7341.	2.5	8
137	Near-interface Si substrate 3d metal contamination during atomic layer deposition processing detected by electron spin resonance. Journal of Applied Physics, 2012, 111, .	2.5	8
138	Silicene nanoribbons on transition metal dichalcogenide substrates: Effects on electronic structure and ballistic transport. Nano Research, 2016, 9, 3394-3406.	10.4	8
139	Leakage current induced by surfactant residues in self-assembly based ultralow-k dielectric materials. Applied Physics Letters, 2017, 111, .	3.3	8
140	Doping-induced ferromagnetism in InSe and SnO monolayers. Journal of Computational Electronics, 2021, 20, 88-94.	2.5	8
141	Blockage of the annealing-induced Si/SiO2 degradation by helium. Applied Physics Letters, 1999, 74, 1009-1011.	3.3	7
142	Comment on "Do Pb1 centers have levels in the Si band gap? Spin-dependent recombination study of the Pb1 †hyperfine spectrum' ―[Appl. Phys. Lett. 76, 3771 (2000)]. Applied Physics Letters, 2001, 78, 145	1-1452.	7
143	Internal photoemission of electrons from Ta-based conductors into SiO2 and HfO2 insulators. Journal of Applied Physics, 2008, 104, .	2.5	7
144	Electron energy band alignment at the NiO/SiO2 interface. Applied Physics Letters, 2010, 96, .	3.3	7

#	Article	IF	CITATIONS
145	Electron band alignment at the interface of (100)GaSb with molecular-beam deposited Al2O3. Applied Physics Letters, 2011, 98, 072102.	3.3	7
146	Oxygen and hydroxyl adsorption on MS ₂ (M = Mo, W, Hf) monolayers: a firstâ€principles molecular dynamics study. Physica Status Solidi - Rapid Research Letters, 2016, 10, 787-791.	2.4	7
147	Evaluation of the effective work-function of monolayer graphene on silicon dioxide by internal photoemission spectroscopy. Thin Solid Films, 2019, 674, 39-43.	1.8	7
148	First-Principles Study of the Contact Resistance at 2D Metal/2D Semiconductor Heterojunctions. Applied Sciences (Switzerland), 2020, 10, 2731.	2.5	7
149	Structural and vibrational properties of amorphous GeO2 from first-principles. Applied Physics Letters, 2011, 98, .	3.3	6
150	Interface nature of oxidized single-crystal arrays of etched Si nanowires on (100)Si. Applied Physics Letters, 2012, 100, 082110.	3.3	6
151	Trap Generation in Buried Oxides of Siliconâ€onâ€Insulator Structures by Vacuum Ultraviolet Radiation. Journal of the Electrochemical Society, 1997, 144, 749-753.	2.9	5
152	Band Alignment at Interfaces of Oxide Insulators with Semiconductors. Integrated Ferroelectrics, 2011, 125, 53-60.	0.7	5
153	Large Area Carbon Nanosheet Capacitors. ECS Solid State Letters, 2014, 3, N8-N10.	1.4	5
154	Band alignment and effective work function of atomic-layer deposited VO2 and V2 O5 films on SiO2 and Al2 O3. Physica Status Solidi C: Current Topics in Solid State Physics, 2015, 12, 238-241.	0.8	5
155	Band offsets and trap-related electron transitions at interfaces of (100)InAs with atomic-layer deposited Al2O3. Journal of Applied Physics, 2016, 120, 235701.	2.5	5
156	Hydrogen induced dipole at the Pt/oxide interface in MOS devices. Physica Status Solidi (A) Applications and Materials Science, 2016, 213, 260-264.	1.8	5
157	Nitrogen acceptor in 2H-polytype synthetic MoS2 assessed by multifrequency electron spin resonance. Journal of Vacuum Science and Technology A: Vacuum, Surfaces and Films, 2018, 36, .	2.1	5
158	Measurement of direct and indirect bandgaps in synthetic ultrathin MoS2 and WS2 films from photoconductivity spectra. Journal of Applied Physics, 2021, 129, .	2.5	5
159	Depth Profiling of Oxygen Vacancy Defect Generation in Buried SiO ₂ . Materials Research Society Symposia Proceedings, 1992, 284, 299.	0.1	4
160	Characterization of S centers generated by thermal degradation in SiO2 on (100)Si. Applied Physics Letters, 2002, 80, 4753-4755.	3.3	4
161	Misfit point defects at the epitaxial Lu2O3/(111)Si interface revealed by electron spin resonance. Applied Physics Letters, 2008, 93, 103505.	3.3	4
162	Comparative electron spin resonance study of epi-Lu2O3/(111)Si and a-Lu2O3/(100)Si interfaces: Misfit point defects. Journal of Applied Physics, 2010, 107, 094502.	2.5	4

#	Article	IF	CITATIONS
163	Electronic structure of NiO layers grown on Al2O3 and SiO2 using metallo-organic chemical vapour deposition. Journal of Applied Physics, 2011, 110, .	2.5	4
164	Band alignment at interfaces of amorphous Al2O3 with Ge1â^'xSnx- and strained Ge-based channels. Applied Physics Letters, 2014, 104, 202107.	3.3	4
165	Modulation of electron barriers between Ti <scp>N</scp> _{<i>x</i>} and oxide insulators (<scp>S</scp> i <scp>O</scp> ₂ , Al ₂ <scp>O</scp> ₃) using Ti interlayer. Physica Status Solidi (A) Applications and Materials Science, 2014, 211, 382-388.	1.8	4
166	Generation of Si dangling bond defects at Si/insulator interfaces induced by oxygen scavenging. Physica Status Solidi (B): Basic Research, 2014, 251, 2193-2196.	1.5	4
167	Impact of strain on the passivation efficiency of Ge dangling bond interface defects in condensation grown SiO2/GexSi1â^'x/SiO2/(100)Si structures with nm-thin GexSi1â^'x layers. Applied Surface Science, 2014, 291, 11-15.	6.1	4
168	Variations of paramagnetic defects and dopants in geo-MoS2 from diverse localities probed by ESR. Journal of Chemical Physics, 2020, 152, 234702.	3.0	4
169	The Nitrogen Acceptor in 2Hâ€Polytype Synthetic MoS ₂ : Frequency and Temperature Dependent ESR Analysis. Physica Status Solidi C: Current Topics in Solid State Physics, 2017, 14, 1700211.	0.8	4
170	Magnetism of neutron-damaged alpha-quartz. Radiation Effects, 1986, 97, 183-190.	0.4	3
171	Impact of supplemental implantation of oxygen on defect centers in the separation by implantation of oxygen structure. Applied Physics Letters, 1995, 67, 1399-1401.	3.3	3
172	Electrical and physical characterization of high-k dielectric layers. , 0, , .		3
173	Influence of metal capping layer on the work function of Mo gated metal-oxide semiconductor stacks. Applied Physics Letters, 2008, 93, 083511.	3.3	3
174	Defects in Low-k Insulators (ΰ=2.5 – 2.0): ESR Analysis and Charge Injection. Materials Research Society Symposia Proceedings, 2011, 1335, 119.	0.1	3
175	Chemical kinetics of the hydrogen-GePb1 defect interaction at the (100)GexSi1â^'x/SiO2 interface. Journal of Vacuum Science and Technology B:Nanotechnology and Microelectronics, 2013, 31, 010603.	1.2	3
176	Determination of energy thresholds of electron excitations at semiconductor/insulator interfaces using trap-related displacement currents. Microelectronic Engineering, 2019, 215, 110992.	2.4	3
177	Pb-type interface defects in (100)Si/SiO2 structures grown in ozonated water solution. Journal of Applied Physics, 2003, 93, 4331-4333.	2.5	2
178	The effect of implanting boron on the optical absorption and electron paramagnetic resonance spectra of silica. Journal of Applied Physics, 2008, 104, 054110.	2.5	2
179	Multi-frequency electron spin resonance study of inherent Si dangling bond defects at the thermal (211)Si/SiO2interface. Physica Status Solidi C: Current Topics in Solid State Physics, 2014, 11, 1589-1592.	0.8	2
180	Thermal stability and temperature dependent electron spin resonance characteristics of the As acceptor in geological 2H-MoS ₂ . Semiconductor Science and Technology, 2019, 34, 035022.	2.0	2

#	Article	IF	CITATIONS
181	Influence of gamma irradiation on ESR active defects in SIMOX structures. , 0, , .		1
182	Hydrogen Induced Positive Charging of Buried SiO/sub 2/. , 0, , .		1
183	Correlation Between Development of Leakage Current and Hydrogen Ionization in Ultrathin Silicon Dioxide Layers. Materials Research Society Symposia Proceedings, 1999, 592, 203.	0.1	1
184	Annealing Induced Degradation of Thermal SiO2On (100)Si: Point Defect Generation. Radiation Effects and Defects in Solids, 2003, 158, 419-425.	1.2	1
185	Charge transition level of GeP _{b1} centers at interfaces of SiO ₂ /Ge _{<i>x</i>} Si _{1â^'<i>x</i>} /SiO ₂ heterostructures investigated by positron annihilation spectroscopy. Physica Status Solidi (B): Basic Research, 2014, 251, 2211-2215.	1.5	1
186	Electron energy distribution in Si/TiN and Si/Ru hybrid floating gates with hafnium oxide based insulators for charge trapping memory devices. Physica Status Solidi (A) Applications and Materials Science, 2016, 213, 265-269.	1.8	1
187	First-principles investigation of defects at GaAs/oxide interfaces. Materials Science in Semiconductor Processing, 2016, 42, 239-241.	4.0	1
188	Internal photoemission of electrons from 2D semiconductor/3D metal barrier structures. Journal Physics D: Applied Physics, 2021, 54, 295101.	2.8	1
189	Buried oxide inhomogeneity in low-dose SIMOX structures. , 0, , .		Ο
190	Localization and Electric-Field Modulated Electron Spin Resonance of a Shallow Donor in Simox. Materials Research Society Symposia Proceedings, 1992, 284, 573.	0.1	0
191	[100]Si with ultrathin layers of SiO/sub 2/, Al/sub 2/O/sub 3/, and ZrO/sub 2/: electron spin resonance study. , 0, , .		Ο
192	Microcharacterization of Defects Induced in Fused Silica by High Power 3ω UV (355nm) Laser Pulses. Microscopy and Microanalysis, 2001, 7, 496-497.	0.4	0
193	Probing Semiconductor/Insulator Heterostructures Through Electron Spin Resonance of Point Defects: Interfaces, Interlayers, and Stress. Materials Research Society Symposia Proceedings, 2006, 984, 1.	0.1	Ο
194	Analysis of the (100)Si/LaAlO3 structure by electron spin resonance: nature of the interface. Journal of Materials Science: Materials in Electronics, 2007, 18, 735-741.	2.2	0
195	Inelastic electron tunneling spectroscopy of HfO2 gate stacks: A study based on first-principles modeling. Applied Physics Letters, 2011, 99, 132101.	3.3	Ο
196	Inherent interface defects in thermal (211)Si/SiO2:29Si hyperfine interaction. , 2014, , .		0
197	(Invited) Nature of Point Defects at High-Mobility Semiconductor/Interfaces Probed by Electron Spin Resonance: Thermal GaAs/GaAs-Oxide Structures. ECS Transactions, 2014, 64, 293-299.	0.5	0
198	Processing-induced near-interfacial thermal donor generation in (100)Si/Si-oxycarbide insulator structures revealed by electron spin resonance. Physica Status Solidi C: Current Topics in Solid State Physics, 2014, 11, 1574-1577.	0.8	0

#	Article	IF	CITATIONS
199	Effect of La doping on interface barrier between Si-passivated Ge and insulating HfO2. Physica Status Solidi C: Current Topics in Solid State Physics, 2016, 13, 855-859.	0.8	Ο
200	Dangling bond defects in silicon-passivated strained-Si1â^'xGex channel layers. Journal of Materials Science: Materials in Electronics, 2020, 31, 75-79.	2.2	0
201	Contact resistance at 2D metal/semiconductor heterostructures. Frontiers of Nanoscience, 2020, 17, 127-140.	0.6	Ο